Accelerated Electromagnetic Simulation of Graphene-Based EEG Probes for MRI Compatibility Using the Huygens' Box Method

Suchit Kumar¹, Samuel M. Flaherty², Alejandro Labastida-Ramírez², Anton Guimerà Brunet³, Ben Dickie⁴, Rob C. Wykes^{1,2}, Kostas Kostarelos², Louis Lemieux^{1*}

¹University College London Queen Square Institute of Neurology, London, UK ²Centre for Nanotechnology in Medicine & Division Neuroscience, University of Manchester, UK ³Centro de Investigación Biomédica en Red en Bioingeniería, Biomateriales y Nanomedicina (CIBER-BBN), Madrid, Spain ⁴Division of Informatics, Imaging and Data Sciences, University of Manchester, Manchester, UK

Introduction

- **Background & Motivation**
 - 1. Concurrent EEG-fMRI captures both electrical brain activity and hemodynamic changes, providing critical insights into brain states [1].
 - 2. Challenges with conventional EEG probes:
 - Metal-based EEG probes introduce MRI artifacts.
 - Safety concerns include RF-induced heating and displacement [2-4].
 - 3. Graphene-based Solution-Gated Field-Effect Transistors (gFETs) offer a promising alternative:
 - Provide **high-fidelity**, **DC-coupled recordings** with minimal interference [5,6].
 - However, their MRI compatibility remains largely unexplored.

- Computational Challenges & Study Aim
 - 4. Computational electromagnetic (EM) simulations are crucial for evaluating MRI compatibility. However, they are computationally expensive due to the probes' submicrometric structures [7].
 - 5. Study Objective:
 - Optimize EM Simulations: Utilize the Huygens' Box (HB) method to improve the efficiency of computational EM simulations while maintaining high spatial resolution.
 - Evaluate Probe Designs: Assess the feasibility of two graphene-based probe designs: intracortical and epicortical, for safe and artifact-free EEG-fMRI integration.
- Ensure RF Safety: Investigate the interaction between the probes and the MRI environment to ensure RF safety and minimize interference.

Methods

- Simulation Setup
 - Software: Sim4Life (V8.0, ZMT) using a Finite-Difference Time-Domain (FDTD) solver [8].
 - Model: A 3D rodent model comprising 68 tissues [9].
 - A Gaussian excitation signal at 300 MHz with a 625 MHz bandwidth was applied.
 - 1. Multi-port method: A two-port configuration was used followed by impedance matching, combining results in circularly polarized mode.
 - 2. Huygens' Box (HB) Method:
 - Step 1: RF coil excitation generated fields within the Huygens' box without the rodent or probe.
 - Step 2: The box was used as the excitation source with the rodent model, both with and without probes.

RF Coil & Probe Modeling

- The RF coil is a two-port high-pass birdcage design with eight rungs, 72 mm diameter/length, 90 mm shield diameter, 225 mm shield length, 9.9 mm rung width, and a 13.8 pF capacitor for 300 MHz resonance.
- The CAD models of graphene-based probes were generated from 2D drawings and converted into multi-layered 3D models with thicknesses of 11.96 µm (intracortical) and 9.84 µm (epicortical).

- Key parameters included the transmit RF field (B₁⁺) and SAR values.
- SAR values were averaged over 0.01 g, 0.1 g, and 1 g tissue, following IEC safety

EM Field Estimations

guidelines [10].

Key Findings

1. Results

- The HB method significantly reduced computation time while achieving higher spatial resolution compared to the multi-port method.
- B₁⁺ field distributions were similar across both methods, with a localized 15–20% **increase** near the probes due to induced currents (Figure 2).
- SAR analysis confirmed localized heating but remained within acceptable safety limits (Table 1).

2. Discussion

- The HB approach enhances EM simulation efficiency and resolution, particularly around the probes and the rodent model.
- However, the absence of the RF coil's impedance matching in the HB method introduces slight uncertainties.
- **SAR elevation** near graphene-based probes remains modest and within safety thresholds.

3. Conclusions

- This study demonstrates the feasibility of using the HB method for efficient EM simulations of graphene-based EEG probes in MRI.
- Findings indicate minimal impact on RF transmission and SAR deposition, ensuring MR compatibility.
- Future work should focus on optimizing computational efficiency, experimental validation, and assessing electrophysiological performance in MRI settings.

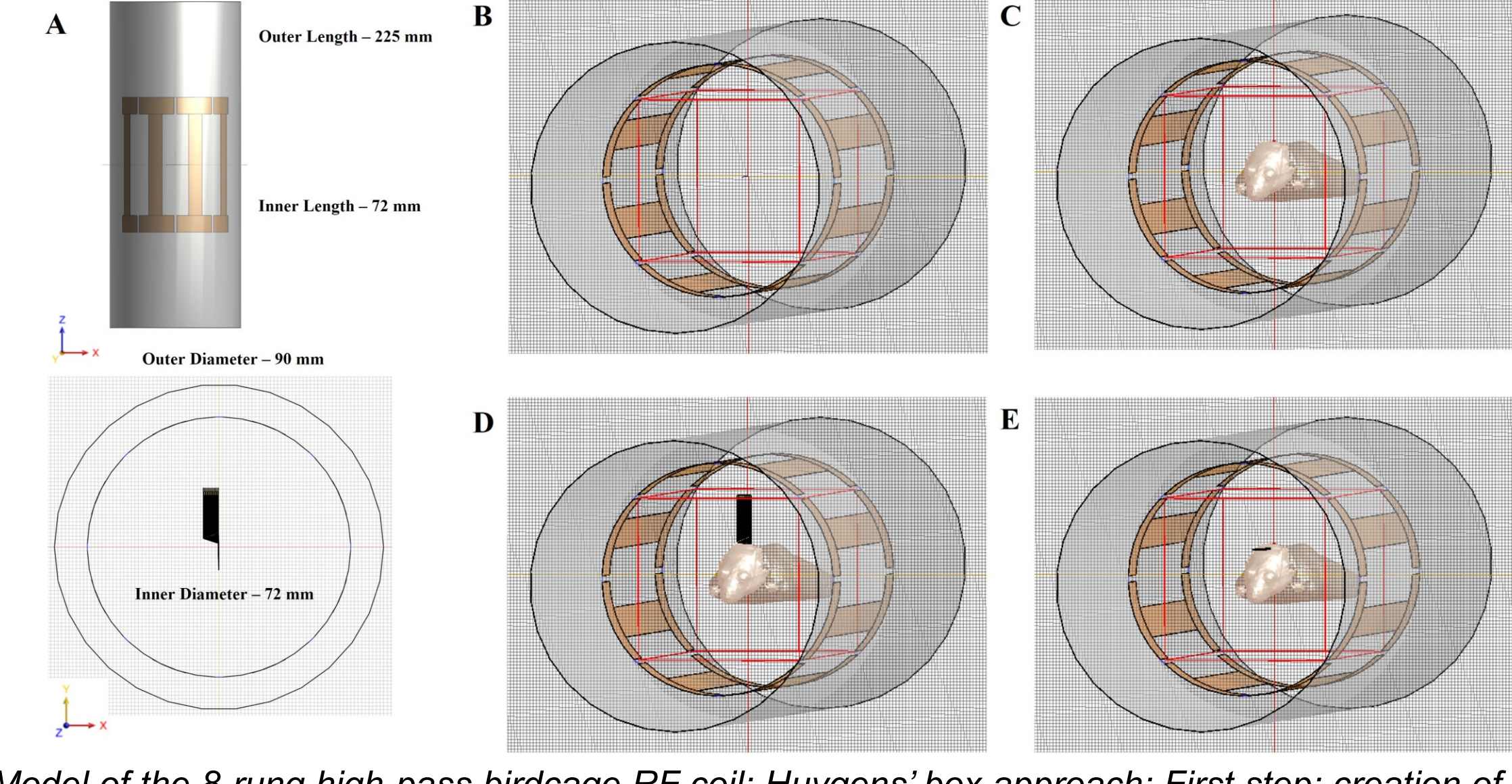


Fig. 1 (A) Model of the 8-rung high-pass birdcage RF coil; Huygens' box approach: First step: creation of the Huygens' source, (B) with the RF coil acting as the source and the red box indicating the region of interest for the Huygens' box; Second step: Implementation of the Huygens' source with the rat and probe models placed inside the Huygens' box; (C) Rat model (without probe); (D) Rat model with intracortical probe; (E) Rat model with epicortical probe.

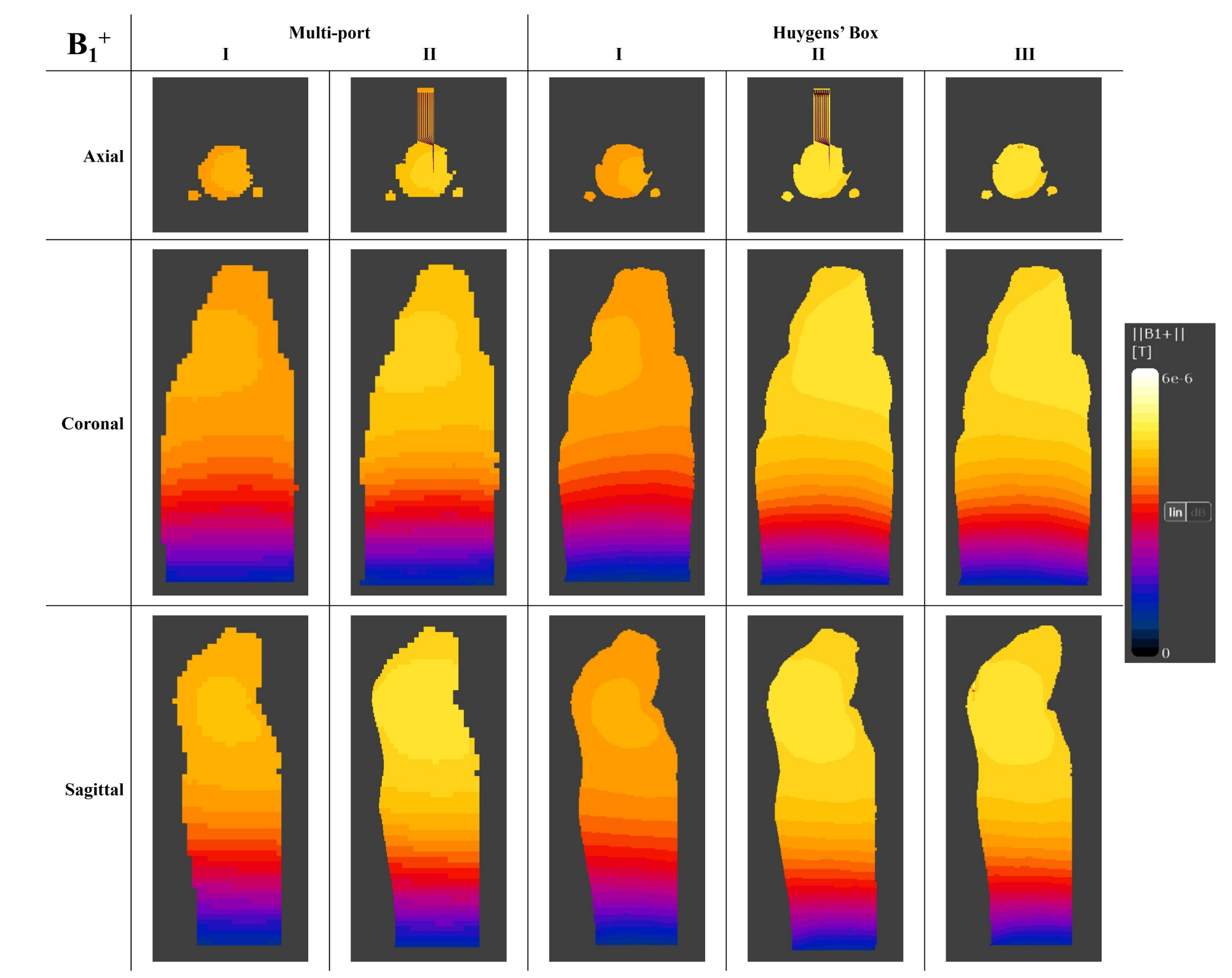


Fig. 2 Simulated B₁+-field distribution in the rodent model for the multi-port approach: (I) without and (II) with intracortical probe; and for the HB approach: (I) without, (II) with intracortical, and (III) with epicortical probe models in axial, coronal, and sagittal views. Values normalized to an input power of 1 watt.

Tissue mass		0.01g	0.1g	1g
A.I	Mass-avg SAR (watt/kg)		0.5393	
	Peak spatial-avg SAR (watt/kg)	2.1462 (Skin)	1.2138 (Muscle, Spleen, Fat, Skin)	0.7720 (Skin)
A.II	Mass-avg SAR (watt/kg)		0.5584	
	Peak spatial-avg SAR (watt/kg)	2.4745 (Fat, Skin)	1.6784 (Liver, Muscle, Fat, Cartilage)	0.8927 (Kidney, Spleen, Spinal Cord, CSF. Liver, Muscle, Fat, Skin)
B.I	Mass-avg SAR (watt/kg)		0.5602	
	Peak spatial-avg SAR (watt/kg)	4.9579 (Intestine)	2.6610 (Intestine)	1.1717 (Skin)
B.II	Mass-avg SAR (watt/kg)		0.6412	
	Peak spatial-avg SAR (watt/kg)	7.7562 (Muscle)	3.939 (Fat, Muscle, Intestine)	1.4852 (Skin)
B.III	Mass-avg SAR (watt/kg)	0.7061		
	Peak spatial-avg SAR (watt/kg)	8.5729 (Muscle)	4.2063 (Fat, Muscle, Intestine)	1.619 (Skin)

Table 1 Mass-averaged SAR for 0.01g, 0.1g, and 1g tissue mass and peak spatial-averaged SAR values for (A) multi-port approach; (B) HB approach.

References: 1] Lemieux et al. Neuroimage. 2001. 2] Stevens et al. J Magn Reson Imaging. 2007. 3] Lemieux et al. Magn Reson Med. 1997. 4] Erhardt et al. J Neural Eng. 2018. 5] Bonaccini Calia et al. Nat Nanotechnol. 2022. 6] Masvidal-Codina et al. Nat Mater. 2019. 7] Neufeld et al. Phys Med Biol. 2009. 8] Sim4Life, ZMT. http://www.zurichmedtech.com. 9] Kainz et al. Phys Med Biol. 2006. 10] IEC 60601-2-33:2022.

Acknowledgements: This project is funded by the EPSRC under grant no. EP/X013669/1. The authors are grateful for the support from Sim4life, ZMT for providing the science license.

